Van Steveninck, R. F. M., & Van Steveninck, M. E. (1983) in *Abscisic Acid* (Addicott, F. T., Ed.) pp 171-235, Praeger, New York.
Venis, M. (1985) *Hormone Binding Sites In Plants*, Longman, New York.
Wassall, S. R., Hester, P., & Stillwell, W. (1985a) *Biochim. Biophys. Acta 815*, 519-522.
Wassall, S. R., Brengle, B., & Stillwell, W. (1985b) *Curr. Top. Plant Biochem. Physiol. 4*, 221.
Wassall, S. R., Phelps, T. M., Albrecht, M. R., Langsford, C. A., & Stillwell, W. (1988) *Biochim. Biophys. Acta 939*, 393-402.
Weinstein, J. N., Yoshikami, S., Henkart, P., Blumenthal, R., & Hagins, W. A. (1977) *Science 195*, 489-491.
Zeevaart, J. A. D., & Creelman, R. A. (1988) *Annu. Rev. Plant Physiol. Plant Mol. Biol. 39*, 439-473.

^{31}P NMR Spectra of Ethidium, Quinacrine, and Daunomycin Complexes with Poly(adenylic acid)·Poly(uridylic acid) RNA Duplex and Calf Thymus DNA†

David G. Gorenstein*,‡ and Kofen Lai§

Department of Chemistry, Purdue University, West Lafayette, Indiana 47907, and University of Illinois at Chicago, Chicago, Illinois 60680

Received October 6, 1988; Revised Manuscript Received December 14, 1988

ABSTRACT: ^{31}P NMR provides a convenient monitor of the phosphate ester backbone conformational changes upon binding of the intercalating drugs ethidium, quinacrine, and daunomycin to sonicated poly(A)·poly(U) and calf thymus DNA. ^{31}P chemical shifts can also be used to assess differences in the duplex unwinding angles in the presence of the drug. Thus a new ^{31}P signal, 1.8–2.2 ppm downfield from the double-stranded helix signals, is observed in the ethidium ion–poly(A)·poly(U) complex. This signal arises from phosphates which are in perturbed environments due to intercalation of the drug. This is in keeping with the hypothesis that the P–O ester torsional angle in phosphates linking the intercalated base pairs is more trans-like. Similar though smaller deshielding of the ^{31}P signals is observed in sonicated poly(A)·poly(U)–quinacrine complexes as well as in the daunomycin complexes. The effect of added ethidium ion, quinacrine, and daunomycin on the ^{31}P spectra of sonicated calf thymus DNA is consistent with Wilson and Jones' (1982) earlier study. In these drug–DNA complexes the drug produces a gradual downfield shift in the DNA ^{31}P signal without the appearance of a separate downfield peak. These differences are attributed to differences in the rate of chemical exchange of the drug between free and bound duplex states. The previous correlation of ^{31}P chemical shift with drug duplex unwinding angle (Wilson & Jones, 1982) is confirmed for both the RNA and DNA duplexes.

It is now widely appreciated that duplex DNA and RNA can exist in a number of different conformations (Saenger, 1984). Significant conformational differences can exist globally along the entire double helix, as in the A-, B-, C-, and Z-forms of DNA. In addition, local conformational heterogeneity in the sugar–phosphate backbone has been most recently noted in the form of sequence-specific variations (Calladine, 1982; Dickerson, 1983) or as the result of drug (Saenger, 1984) or protein binding (Anderson et al., 1987) to local regions of the poly(nucleic acids).

While ^{1}H NMR can provide detailed information on the overall conformation of the sugar rings and bases of oligonucleotides, it generally is unable to provide very much information on the conformation of the phosphate ester backbone. Of the six torsional angles that largely define the backbone structure, only the four involving the sugar ring are amenable to analysis by ^{1}H NMR techniques (via coupling constant or NOESY distance measurements). It has been suggested that the sugar ring and base form a rather rigid unit with the main conformational flexibility of the nucleic acid backbone being limited to the two P–O phosphate ester torsional angles (Sundaralingam, 1969). Thus, one of these, the C3′–O3′–P–O5′ torsional angle, ζ, is found to be the most variable one in the B-form of the DNA double helix, and the other, the O3′–P–O5′–C5′ torsional angle, α, is one of the most variable in the A-form of the RNA or DNA duplex (Saenger, 1984). Indeed, following the original suggestion of Sundaralingam (1969) and on the basis of recent X-ray crystallographic studies of oligonucleotides, Saenger (1984) has noted that the P–O bonds may be considered the "major pivots affecting polynucleotide structure".

We have proposed that ^{31}P NMR spectroscopy is potentially capable of providing information on the most important remaining two torsional angles involving the phosphate ester bonds that define the nucleic acid backbone. Our studies (Gorenstein & Kar, 1975; Gorenstein, 1978, 1981, 1983a,b, 1984) indicated that a phosphate diester monoanion in a gauche,gauche (g,g) conformation (referring to the α and ζ torsional angles) should have a ^{31}P chemical shift 1.5–2.5 ppm upfield from an ester in a non-g,g conformation. Our earlier ^{31}P NMR studies on poly- and oligo(nucleic acids) described in Gorenstein et al. (1976, 1982, 1988), Gorenstein (1978, 1981, 1983a,b, 1984), and Gorenstein and Luxon (1979)

†Supported by NIH (Grants GM36281 and AI27744), the Purdue University Biochemical Magnetic Resonance Laboratory which is supported by NIH (Grant RR01077 from the Biotechnology Resources Program of the Division of Research Resources), and the NSF National Biological Facilities Center on Biomolecular NMR, Structure and Design at Purdue (Grants BBS 8614177 and 8714258 from the Division of Biological Instrumentation).
‡Purdue University.
§University of Illinois at Chicago.

0006-2960/89/0428-2804$01.50/0

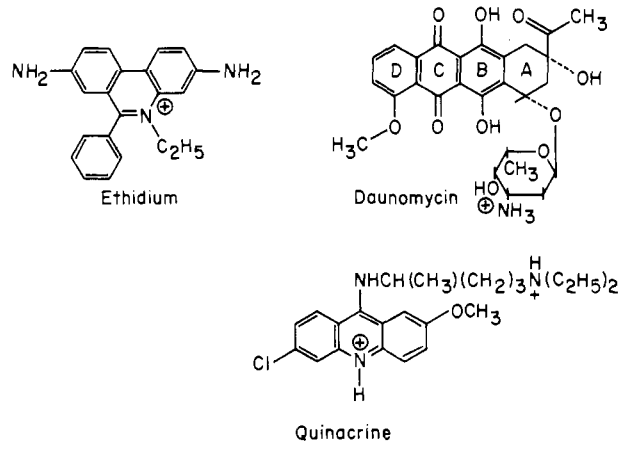

FIGURE 1: Structures of poly(nucleic acid) binding drugs.

confirmed our suggestion that the base-stacked, helical structure with a g,g phosphate ester torsional conformation should be upfield from the random coil conformation.

In a previous study (Goldfield et al., 1983; Gorenstein & Goldfield, 1984) our laboratory has looked at the ^{31}P NMR spectra of the model system poly(adenylic acid)·oligo(uridylic acid) [poly(A)·oligo(U)] in which separate ^{31}P signals are observed for the multistranded poly(A)·oligo(U) helix and the single-strand forms of poly(A) and oligo(U). ^{31}P NMR spectroscopy can monitor the "helix–coil" transition in single- and double-stranded nucleic acids (Chen & Cohen, 1984; Patel & Canuel, 1979; Patel, 1976, 1979a,b; Gorenstein et al., 1976, 1982; Gorenstein, 1978, 1984). A downfield shift at higher temperatures for a wide structural range of nucleic acids has been observed. At low temperature the nucleic acids exist largely in a base-stacked, helical conformation with the phosphate ester predominantly in the g,g conformation, while at higher temperature the nucleic acids will largely exist in random coil, unstacked conformation with the phosphate ester in an increased proportion of non-gauche (i.e., gauche,trans) conformations. We also have examined the binding of a drug, ethidium ion, to poly(A)·oligo(U) (Goldfield et al., 1983; Gorenstein & Goldfield, 1984). Binding of the drug produces a new downfield ^{31}P signal which is induced in poly(A)·oligo(U) by the intercalation of the drug into the duplex.

In this paper, we examine the effect of the binding of ethidium, quinacrine, and daunomycin (structures shown in Figure 1) to sonicated poly(A)·poly(U) and calf thymus DNA. ^{31}P NMR provides a convenient monitor of the phosphate ester conformational change occurring upon binding of drugs to nucleic acids. ^{31}P chemical shifts can also be used to test differences in the unwinding angles[1] in both DNA and RNA double-helix–drug complexes (Jones & Wilson, 1980; Wilson & Jones, 1981, 1982; Wilson et al., 1981; Chandrasekaran et al., 1985).

Experimental Procedures

Materials

Poly(A)·poly(U) was purchased from P-L Biochemicals Co. Calf thymus DNA was obtained from Sigma Chemical Co. Quinacrine dihydrochloride, ethidium bromide, and daunomycin hydrochloride were also purchased from Sigma. ϕX174 *Hae*III and λ *Hin*dIII fragments were from Bethesda Research Laboratory.

Methods

Sonication. Poly(A)·poly(U) and calf thymus DNA were sonicated in the cold room at the maximum output power below cavitation by use of a tapered probe of a Branson Model 350 sonicator. Solutions were 2–4 mL in 0.1 or 0.2 M NaCl buffer contained in a thick-walled glass tube equipped with a nitrogen gas flow. The temperature was adjusted as far as possible between 0 and 4 °C, by use of an ice bath and by use of the pulse control with 50% duty cycle. After a 2-h sonication time, samples were centrifuged at 15000 rpm for at least 30 min at 4 °C.

Size Determination. Polyacrylamide gel electrophoresis was carried out on a slab gel apparatus according to the procedure of Maniatis et al. (1975) and Cohen et al. (1981). Materials for gel electrophoresis were obtained from Bio-Rad. Sonicated DNA or RNA molecules were examined on slab gels (20 cm × 15 cm × 0.2 cm) in Tris–borate–EDTA (TBE) buffer [0.09 M Tris–borate (pH 8.3), 2.5 mM EDTA]. Samples were ethanol precipitated prior to electrophoresis to remove salt and buffer; 0.1 volume of 3 M sodium acetate and 2 volumes of 95% ethanol were added to the sample; the mixture was placed on powdered dry ice for 5 min and centrifuged at top speed in an Eppendorf microcentrifuge for 5 min. The precipitate was rinsed two times with 95% cold ethanol and resuspended in 25 μL of ten times diluted electrophoresis TBE buffer containing 50% glycerol, 0.025% xylene cyanol FF, and 0.025% bromophenol blue. Electrophoresis was carried out at room temperature at constant voltage (150 V). Standards for size determination were ϕX174 RF *Hae*III and λ *Hin*dIII fragments. Bands were visualized by staining with ethidium bromide (0.001%). A microdensitometer was used to scan the gel film. The gels indicated that sonication of the DNA and duplex RNA yielded fragments in the general range of 150–200 base pairs. To test for small fragments (<10 bp) in the products of sonication, aliquots were treated with cold perchloric acid (5%) for 1 h and centrifuged (Cohen et al., 1981). UV measurements on a Varian 210 spectrophotometer at 260 nm indicated 15–18% small fragments.

^{31}P NMR. Before the ^{31}P NMR spectra were run, all of the sonicated nucleic acids were dialyzed twice against a 1-L solution containing 0.2 M NaCl, 10 mM cacodylate, pH 7.0, 10 mM Na_2EDTA, and 1 mg of Chelex-100 ion-exchange resin for 10–24 h at 4 °C and then dialyzed in the same buffer without Chelex-100 resin and 1 mM Na_2EDTA for 18–24 h. This is to safeguard against contamination of the biochemicals by paramagnetic metal ion impurities, which is especially a problem with sonicated samples. All drug stock solutions were stored at −5 °C until needed. All of the drugs were dissolved in double-distilled water, treated with Chelex-100 resin, and then centrifuged and checked for impurities by TLC, showing only one component to be present. The solvent mixture of TLC for EtBr is 1-butanol–acetic acid–H_2O (3:4:3); for daunomycin and quinacrine it is acetic acid–methanol–chloroform (1:1:8) (Chaires et al., 1982b). The concentrations of drug solutions are measured by UV–vis absorbancy at various wavelengths [ϵ_{510} = 4110 cm^{-1} M^{-1} for EtBr (Jones & Kearns, 1975); ϵ_{424} = 9750 cm^{-1} M^{-1} for quinacrine (Bontemps & Fredericq, 1974); ϵ_{480} = 11 500 cm^{-1} M^{-1} for daunomycin (Chaires et al., 1982a)]. All samples were used immediately or stored at −5 °C if it was used at some later time. The pH of the buffer–nucleic acid solutions was adjusted on a Radiometer Model PHM 64 Research meter to pH 7.0.

[1] In the B-form DNA double helix with ~10 base pairs per turn (360°) of the helix, each base pair is rotated ca. +36° (helix twist) with respect to the nearest-neighbor base pair. Insertion (intercalation) of a drug between the stacked base pairs reduces the normal value of the helix twist, and the amount of the change in the rotation is termed the unwinding angle.

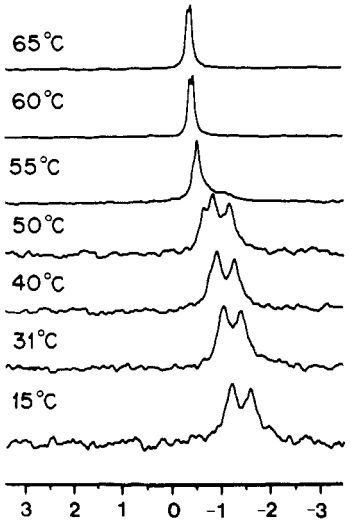

FIGURE 2: ^{31}P NMR spectra of sonicated poly(A)·poly(U) (1:1) at various temperatures in 0.2 M NaCl, 10 mM cacodylate, 1 mM EDTA, pH 7.0, and 20% D_2O buffer at 32.4 MHz. Total nucleotide concentration 10.1 mg/mL. Exponential line broadening 1 Hz.

^{31}P NMR spectra were recorded on a Bruker WP-80 FT NMR spectrometer at 32.38 MHz. For the NMR studies the nucleic acid solution contained 20% D_2O for field locking. All samples were placed in a 5-mm NMR tube. Sample volume was 0.3–0.5 mL with total polynucleotide concentration generally ca. 10.0 mg/mL. ^{31}P NMR spectra were taken with 56° pulses, 4K–8K data points, and 1.02–2.04-s recycle times. The spectra were broad-band ^1H decoupled with the power set at 2 W, and 2.0-Hz line broadening was applied to the FID. The temperature of the sample was controlled to within ±1 °C by a Bruker temperature control unit using nitrogen gas as a coolant.

Chemical shifts are externally referenced to a capillary of 85% phosphoric acid in D_2O at room temperature (25 °C) unless otherwise specified (additional reference is made to a D_2O solution of trimethyl phosphate at 25 °C which is 3.456 ppm downfield of 85% phosphoric acid). Positive chemical shifts are downfield from phosphoric acid. Spin–lattice relaxation times (T_1) were determined by the fast inversion–recovery method as described previously (Gorenstein & Luxon, 1979). Data were analyzed by a nonlinear least-squares method (Dye & Nicely, 1971) on a PDP-11/03 computer.

Results

Poly(A)·Poly(U) without Drugs. The temperature dependence of the ^{31}P NMR spectra and chemical shifts of a sonicated 1:1 mixture of poly(adenylic acid) and poly(uridylic acid) [poly(A)·poly(U)] is shown in Figures 2 and 3. At higher temperature (<55 °C) ^{31}P spectra correspond largely to the superposition of the component poly(A) and poly(U) spectra. Near the melting temperature of the duplex ($T_m \sim$ 48 °C), three signals are possibly present (although this is difficult to firmly establish within the signal to noise of the spectra). At 50 °C, besides the single-strand poly(A) and poly(U), a new upfield signal at −0.84 ppm is reproducibly observed, which we have previously assigned in poly(A)·oligo(U) (Gorenstein et al., 1982) to a double-helix phosphate signal (we are assuming that the additional signal is not attributable to inadequacies in preparation of the 1:1 stoichiometry and that at the 1:1 stoichiometry only double and no triple helices are present—see below). Below the melting temperature, there are two signals (labeled DH_1 and DH_2 in Figure 3) which correspond to two alternating conformations of the backbone phosphates of the double helix (Joseph &

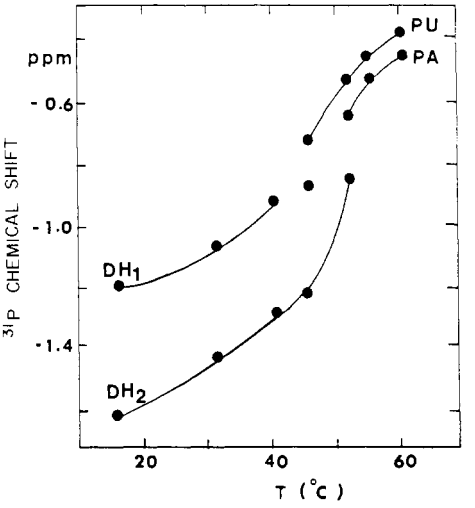

FIGURE 3: ^{31}P chemical shift melting curves for sonicated poly(A)·poly(U) (1:1) signals. See legend to Figure 2.

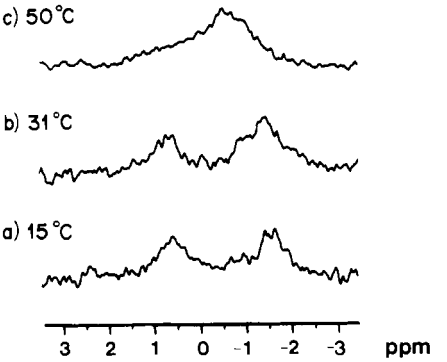

FIGURE 4: ^{31}P NMR spectra of sonicated poly(A)·poly(U)–Etd (1:1:3) at various temperatures in 0.2 M NaCl, 10 mM cacodylate, 1 mM EDTA, pH 7.0, and 20% D_2O buffer, at 32.4 MHz. Exponential line broadening 2 Hz.

Bolton, 1984). The phosphorus double-helical signals below T_m are substantially broader (10–18-Hz line width at half-height) than the single-strand signals (the line width of free single helices at temperatures above T_m is 2–8 Hz). The polymeric, double-stranded helix will be much more rigid than the poly(A) or poly(U) single helix. The rotational correlation time of the duplex will be greatly reduced—this shortens the ^{31}P transverse relaxation time (T_2) and broadens the signals. The longitudinal relaxation times, T_1, measured for a 1:1 sample of sonicated poly(A)·poly(U) at 31 °C, 32.38 MHz, are 2.55 ± 0.11 s for the downfield signal and 2.17 ± 0.17 s for the upfield signal. The T_1 for poly(A) (1.75 s) (Akasaka et al., 1975, 1977) at 32.4 MHz or poly(U) (1.14 s) at 24.3 MHz is less than the T_1's for either of the two phosphate signals of the poly(A)·poly(U) double helix. The ^{31}P chemical shift melting profiles (Figure 3) for these two signals show a sharp melting transition, characteristic of a cooperatively melting multistranded species. All of these results are consistent with the assignments of these signals. To our knowledge these ^{31}P studies represent the first time separate NMR signals for both the double- and single-stranded states have been simultaneously observed in the poly(A)·poly(U) system.

Poly(A)·Poly(U) with Ethidium Ion (Etd). The temperature dependence of the ^{31}P spectra and chemical shifts of sonicated poly(A)·poly(U) with added ethidium ion (1:1:3) is shown in Figures 4 and 5. In the presence of Etd ion we observe a new downfield peak at 0.6 ppm (Figure 4). It appears approximately 1.8–2.2 ppm downfield from the double-stranded helix signals. The downfield drug/helix peak

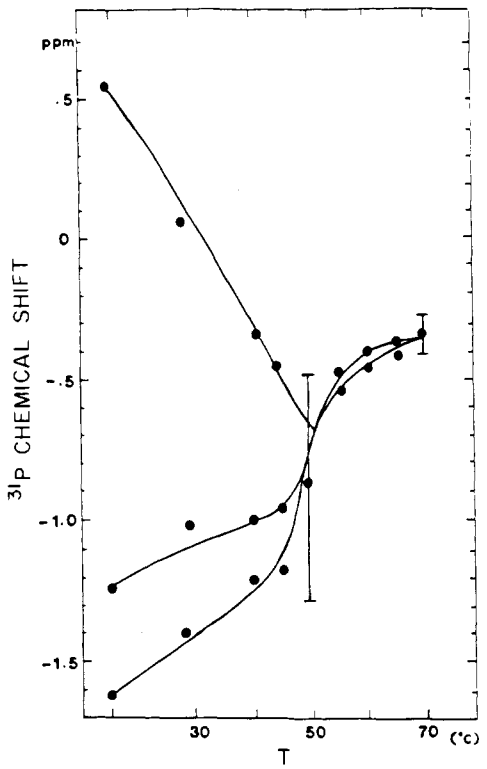

FIGURE 5: ^{31}P melting curves for signals in Figure 4 [sonicated poly(A)·poly(U)–Etd]. Conditions the same as in Figure 4.

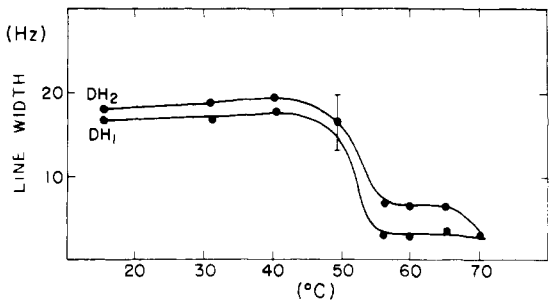

FIGURE 6: Plot of the corrected line widths at half-height at 32.4 MHz vs various temperatures for signals in Figure 4 [sonicated poly(A)·poly(U)–Etd].

accounts for ~46% of the total integrated intensity at 15 °C and saturating drug ratios (=[drug]/[duplex] > 1).

As shown in Figures 4 and 5, when the temperature of a saturated (1:1:3) poly(A)·poly(U)–Etd complex is increased up to 50 °C, the downfield, intercalating drug/helix signal disappears and coalesces with the upfield signal(s) to form a single very broad peak. The temperature dependence to the line width of this complex is shown in Figure 6. There is a sharp decrease in line width of this complex above 52 °C. Increasing the ratio of drug/poly(A)·poly(U) between drug ratios of 0.3 and 3.0 (data not shown) has little effect on the ^{31}P chemical shift of the three signals at 15 °C. However, the line widths of the signals increase from 10 to 22–30 Hz with increasing [drug]/[RNA] ratios (Figure 7). At higher ratios the two upfield peaks are too broad to resolve.

DNA with Etd Ion. Adding ethidium ion to sonicated calf thymus DNA shifts the single ^{31}P signal gradually downfield (Figure 1 of supplementary material; an example of the spectrum at saturating ratio of ethidium is shown in Figure 8b). In confirmation of the results of Jones and Wilson (1980) and Levy et al. (1984), we do not observe any decrease in intensity of the ^{31}P signal with increasing ethidium, as reported by Hogan and Jardetzky (1980). At saturating drug ratios

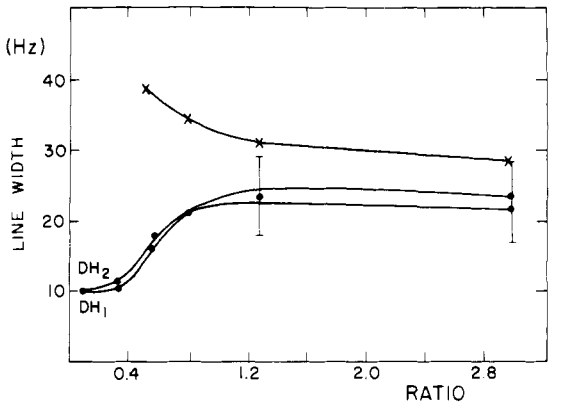

FIGURE 7: Plot of the corrected line widths at half-height at 32.4 MHz for poly(A)·poly(U)–Etd at various molar ratios of Etd, in 0.2 M NaCl 10 mM cacodylate, and 1 mM EDTA buffer, 15 °C, at 32.4 MHz. Exponential line broadening 2 Hz. (●) Upfield duplex signals; (×) downfield intercalated drug site signal.

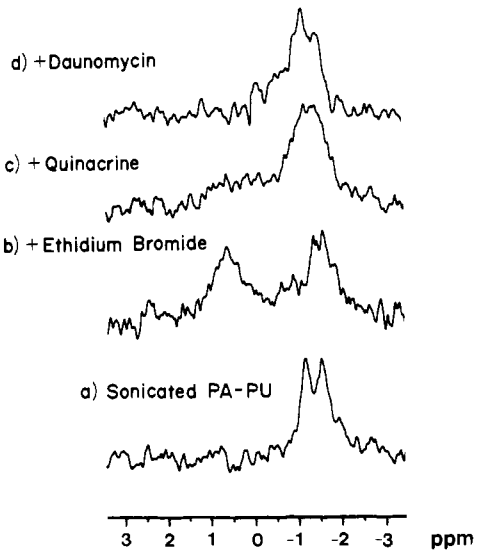

FIGURE 8: ^{31}P NMR spectra of sonicated calf thymus DNA with and without drugs. (a) Sonicated calf thymus DNA; (b) plus ethidium (1:0.91); (c) plus quinacrine (1:0.58); (d) plus daunomycin (1:0.62). Under the same conditions as in Figure 7.

the signal is shifted downfield by 0.66 ppm—quite comparable to the shift observed by Wilson and Jones (1982) of 0.62 ppm. The ethidium increases the line width of this DNA–drug complex by approximately 36 Hz at saturating drug ratios ([drug]/[DNA] > 0.4).

Poly(A)·Poly(U) with Quinacrine. The temperature dependence of the ^{31}P spectra and chemical shifts of a sonicated poly(A)·poly(U)–quinacrine (1:1:1.3) complex are shown in Figures 2 and 3 of the supplementary material; an example of the spectrum at saturating ratio of quinacrine is shown in Figure 9c. At 15 °C the two poly(A)·poly(U) double-helix main signals coalesce to form one broadened peak, and a very broad downfield shoulder to the main peak appears around 0.3 ppm (Figure 9c). The quinacrine–RNA downfield signal sharpens from 40 to 10 Hz over the temperature range of 20–60 °C, respectively. Quinacrine broadens the double-helix signals by ca. 10 Hz with increasing intercalator concentration, in a manner similar to that of ethidium. In contrast to the behavior of ethidium, the ^{31}P chemical shifts of the quinacrine–duplex complex change very little with increasing drug/duplex ratios.

DNA with Quinacrine. Increasing quinacrine/DNA ratios shift the single ^{31}P signal gradually downfield until a ratio of 0.4–0.5 is achieved, after which no further changes are evident

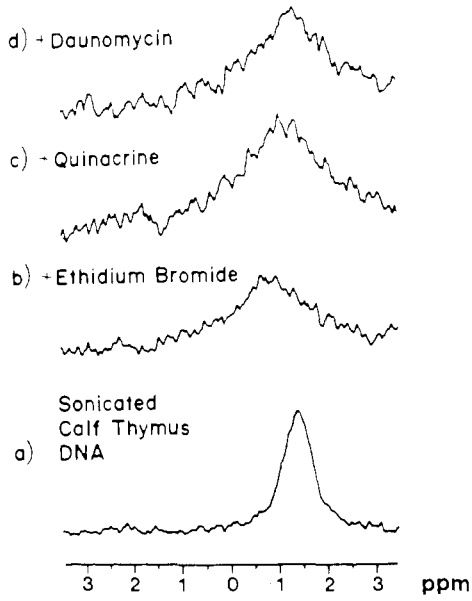

FIGURE 9: ^{31}P NMR spectra of sonicated poly(A)·poly(U) with and without drugs. (a) Sonicated poly(A)·poly(U) (1:1); (b) plus ethidium (1:1:3); (c) plus quinacrine (1:1:1.26); (d) plus daunomycin (1:1:0.51). Under the same conditions as in Figure 7.

(an example of the spectrum at a saturating ratio of quinacrine is shown in Figure 8c). We observe a maximum shift of 0.34 ppm, quite comparable to Wilson and Jones' (1982) value of 0.40 ppm. The quinacrine produces line broadening which increases as a function of intercalator concentration in a manner very similar to that of ethidium. Thus the DNA ^{31}P signal line width at 15 °C increases approximately 30–35 Hz at saturating levels of the intercalator.

Poly(A)·Poly(U) with Daunomycin. A downfield shoulder to the main signal (−1 ppm) is also observed in the poly(A)·poly(U)–daunomycin sample (Figure 4 of the supplementary material; see Figure 9d for an example of the spectra at saturating drug ratios). The temperature dependence of the ^{31}P chemical shifts of this complex (plot not shown) shows that this complex has a higher melting temperature ($T_m \sim 56$ °C) than poly(A)·poly(U) ($T_m \sim 50$ °C). The signals sharpen with increasing temperature (Figure 4 of the supplementary material). At increasing ratios of drug/poly(A)·poly(U), there is little change in the ^{31}P chemical shifts while the signal broadens from 10 to 22 Hz and then levels off with no further increase at drug/DNA ratios of >0.2.

DNA with Daunomycin. Addition of a saturating ratio of daunomycin (ratios > 0.4) produces a 0.11-ppm downfield shift in the DNA ^{31}P signal (Figure 8d); Wilson and Jones (1982) observed a comparable shift of 0.16 ppm. The magnitude of the total shift is smaller than that of ethidium ion or quinacrine. The line width of the drug–DNA ^{31}P NMR signal at 15 °C increases approximately 45–50 Hz upon addition of a saturating ratio of daunomycin. Increasing the temperature from 15 to 70 °C decreases the line width of the daunomycin–DNA ^{31}P signal from 72 to 20 Hz, respectively (data not shown).

Correlation of ^{31}P Chemical Shifts with Helix Unwinding Angles and Helix Twist. Wilson and Jones (1982) have noted that the ^{31}P chemical shifts of the drug–DNA complexes are linearly correlated to the observed degree of unwinding of the duplex DNA upon drug binding. Our own results corroborate their observations. Shown in Figure 10 is a plot of the calculated helix twist of the drug–DNA complexes vs ^{31}P chemical shifts. As discussed below, the helical twist values that we have used in Figure 10 from our data as well as those of

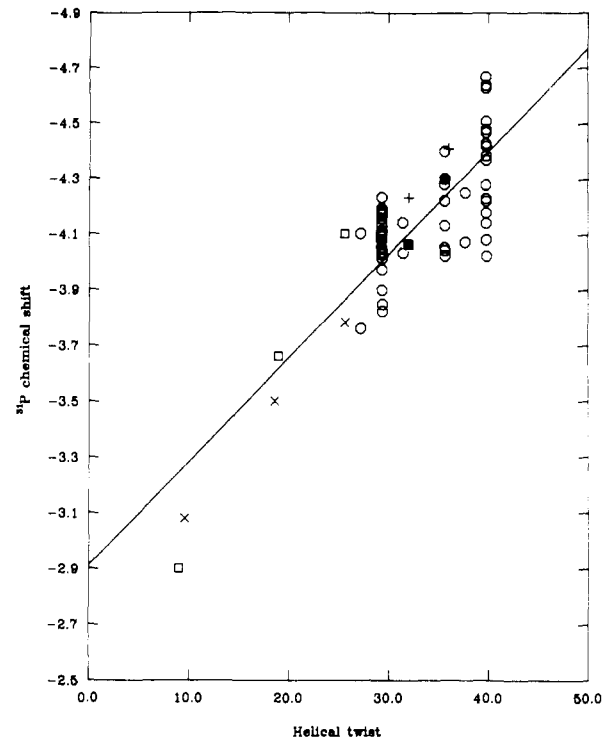

FIGURE 10: Plot of ^{31}P chemical shift vs calculated helix twist, t_g. 10–14 bp oligonucleotide terminal phosphate shifts [(○); t_g derived from $t_g = 35.6 + 2.1\Sigma_1$]. Wilson and Jones' (1982) drug–DNA data (×), drug–calf thymus DNA data from this study (□), and A-DNA (■), B-DNA (△), and alternating poly d(AT) (+) shifts are shown. The helix twist for the drug–DNA complex is calculated from the difference between the helix twist of B-DNA ($t_g = 35.6°$) and the unwinding angle ϕ for the drug–DNA complex (for ethidium, $\phi = 26°$; for quinacrine, $\phi = 17°$; for daunomycin, $\phi = 10°$). The ^{31}P chemical shifts of the drug–DNA complexes have been corrected for chemical shift averaging. ^{31}P chemical shifts are reported relative to trimethyl phosphate which is 3.456 ppm downfield from 85% phosphoric acid.

Wilson and Jones (1982) represent the difference between the normal B-DNA helical twist angle of 35.6° and the observed helical unwinding angle resulting from binding of the drug. Also included in the figure are the ^{31}P chemical shifts and helical twist values of a number of other deoxyribonucleotide duplexes from the literature (see below). If we do a linear least-squares fit of the ^{31}P shifts of the assigned deoxyribonucleotide duplexes and drug–duplex complexes to helical twist, a modest correlation appears to exist between the two parameters. The correlation coefficient (R) between ^{31}P shifts and helical twist is 0.85 (Figure 10).

A similar and rather better correlation is established between ^{31}P chemical shifts of the downfield signal of the three poly(A)·poly(U)–drug complexes and the helical twist for the drug–DNA duplexes (solid line in Figure 11; correlation coefficient $R = 0.95$). Unfortunately, we do not have unwinding angles for binding ethidium, quinacrine, or daunomycin to duplex RNA. We make the assumption in Figure 11 that the unwinding angles for the RNA complexes are comparable to those of the DNA complexes.

Discussion

Our laboratory has suggested that ^{31}P chemical shifts are dependent on P–O ester torsional angles (ζ and α) and O–P–O bond angles. Previous results have suggested that a phosphate diester in a gauche,gauche (g,g) conformation should have a ^{31}P chemical shift ca. 1.5 ppm upfield from that of a phosphate diester in a more extended conformation such a gauche,trans (g,t) (Gorenstein & Kar, 1975; Gorenstein, 1981; Gorenstein

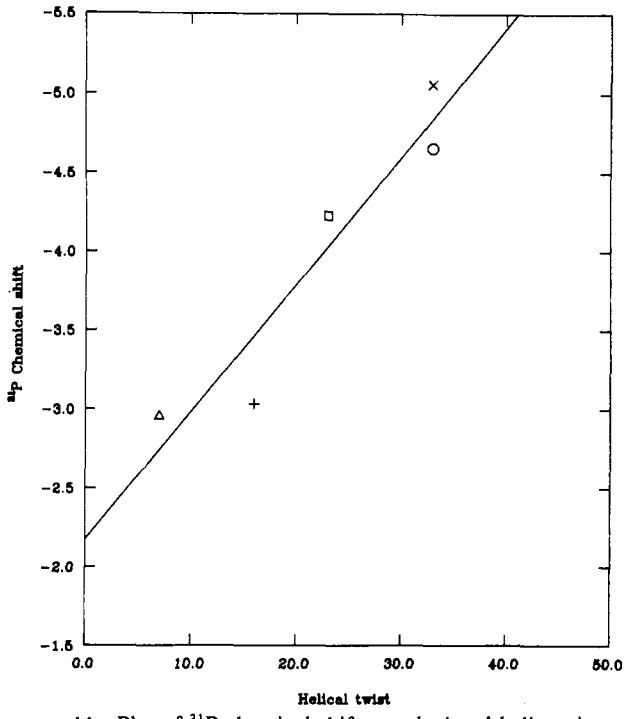

FIGURE 11: Plot of ^{31}P chemical shift vs calculated helix twist, t_g, for poly(A)·poly(U) (×, ○) and various drug–poly(A)·poly(U) complexes at saturating levels of ethidium (△), quinacrine (+), and daunomycin (□). The helix twist is calculated from the difference between the helix twist of poly(A)·poly(U) (33°) and the unwinding angle ϕ for the drug–DNA complex (for ethidium, ϕ = 26°; for quinacrine, ϕ = 17°; for daunomycin, ϕ = 10°). ^{31}P chemical shifts are reported relative to trimethyl phosphate which is 3.456 ppm downfield from 85% phosphoric acid.

& Goldfield, 1984). This hypothesis applies directly to the ^{31}P spectra of nucleic acid–drug complexes.

Patel (1974a–c, 1976) first reported that the intercalating drug actinomycin D (Act D) shifted several phosphate diester signals up to 2.6 ppm downfield from the double-helical signal upon binding to oligonucleotide duplexes containing dGdC base pairs. Thus, downfield shifts of 1.6 and 2.6 ppm in the dCdGdCdG–Act D (2:1) and 1.6 ppm in the pdGdC–Act D (2:1) complexes at 8 °C have been observed. Reinhardt and Krugh (1977) showed that at even lower temperature (−18 °C) in methanol/water the ^{31}P signals of the two phosphates in duplex pdGdC are split into two signals and shifted 1.7 and 2.4 ppm downfield upon complexation with Act D. Similar shifts are also observed in 2:1 Act D–oligonucleotide duplex complexes [cf. Scott et al. (1988)].

These shifts are consistent with the Jain and Sobell (1972) model for these intercalated complexes: partial unwinding of a specific section of the double helix allows these planar, heterocyclic drugs such as Act D to stack between two base pairs. We have also recently shown that the downfield-shifted peak in a d(AGCT)–Act D complex is the dGdC base pair complex by an ^{17}O/^{18}O phosphoryl labeling method [Shah et al., 1984; see also Petersheim et al. (1984)]. X-ray studies on various intercalating drug–duplex complexes (Saenger, 1984; Shieh et al., 1980; Reddy et al., 1979) suggest that the major backbone deformation of the nucleic acid upon intercalation of the drug involves changes in both the P–O and C–O torsional angles (see below). According to the ^{31}P chemical shift calculations, such P–O torsional angle perturbations of 20–120° can result in ^{31}P deshielding of ca. 0.3–1.5 ppm (Gorenstein & Goldfield, 1982; Gorenstein, 1984). Pullman and co-workers (Giessner-Prettre et al., 1984) have suggested that ^{31}P chemical shifts should be a function of the C5′–O5′ and C3′–O3 torsion angles besides the P–O5′ and P–O3′ torsion angles. The observed torsional angle changes for these drug complexes are therefore large enough to explain the observed ^{31}P chemical shift perturbations, such as the 2-ppm downfield shift for poly(A)·poly(U)–Etd.

^{31}P Spectral Changes in Poly(A)·Poly(U). In the absence of added drugs the sonicated poly(A)·poly(U) ^{31}P spectra show two equal intensity signals separated by ca. 0.4 ppm (−1.2 and −1.6 ppm; Figure 4). As shown by Alderfer and Hazel (1981), these signals are associated with the duplex. The chemical shifts of the triplex are +0.07, −0.38, and −0.90 ppm (Alderfer & Hazel, 1981) referenced to 85% phosphoric acid, and hence, none of the triplex form is present in our sample preparation. Joseph and Bolton (1984) have shown by ^{17}O labeling of the phosphates that the two main ^{31}P signals are associated with phosphates in alternating conformations along the duplex poly(A)·poly(U) rather than the phosphates in the two different strands. The separation of the two signals could possibly be attributed to alternating helical twist values along the duplex (presumably an "alternating A-RNA" structure). From utilization of the correlation shown in Figure 11, helix twist values of 31° and 36° could produce such ^{31}P chemical shift differences (see below for additional discussion of this correlation). Thus the measured helix twist value for duplex poly(A)·poly(U) of 33° from X-ray fiber diffraction studies (Arnott et al., 1973) could thus really represent an average of the alternating values.

Klug and co-workers (Scheffler et al., 1968) have suggested that poly[d(AT)] also exists in an "alternating B" conformation. Significantly, the ^{31}P spectrum of poly[d(AT)] gives two signals separated by as much as 0.8 ppm depending upon salt conditions (Shindo et al., 1979). In low-salt solution poly[d(AT)] shows a separation of ^{31}P signals of 0.24 ppm (Shindo et al., 1979). By thiophosphoryl labeling, Eckstein and Jovin (1983) were able to establish that the deshielded ^{31}P signal arises from the TpA phosphates, which on the basis of an X-ray crystal model are in a more extended trans-like phosphate ester conformation. The ^{31}P signal of the ApT phosphates is quite similar to that of a normal B-DNA phosphate and indeed is in a g^-,g^- conformation. According to our ^{31}P chemical shift/helical twist correlation of Figure 10, this downfield TpA phosphate signal suggests an alternating helical twist of ~32° and 36° for the TpA and ApT portions of the duplex, respectively, consistent with the X-ray studies. Similarly, the ^{31}P signal of chicken erythrocyte DNA shifts downfield by 0.2–0.3 ppm as it is converted from the B- to the A-DNA conformation (Kypr et al., 1986). A-DNA shows a t_g of ca. 32–34° in contrast to B-DNA with t_g of ca. 36°. These downfield shifts of the TpA phosphate in poly[d(AT)] and in A-DNA phosphates are thus in agreement with the helical twist dependence to ^{31}P chemical shifts. It will be interesting to determine whether the poly(A)·poly(U) ^{31}P chemical shift differences do indeed arise from such alternating A-RNA conformations.

^{31}P Spectral Changes in Drug–Poly(A)·Poly(U) Complexes. Titration of the poly(A)·poly(U) ^{31}P spectra with ethidium produces a new signal 1.8–2.2 ppm downfield from the duplex signal. At saturating levels of the drug ([drug]/[DNA] ratios > 0.5), the relative intensity of the downfield signal relative to that of the largely unperturbed upfield signal is ca. 1:1 (most clearly seen in the ethidium ion–duplex spectra at low temperature). The new downfield signal that we observe in the sonicated poly(A)·poly(U)–Etd complex is similar to the downfield signals of the Act D–duplex and poly(A)·oligo(U)–Etd complexes (Shah et al., 1984; Goldfield et al., 1983).

In the poly(A)·poly(U)–quinacrine and poly(A)·poly(U)–daunomycin complexes the new downfield signal appears as a very broad downfield shoulder to the main signal (a comparison of all three complexes under identical conditions is shown in Figure 9).

This deshielding for ca. half of the phosphate signals in the poly(A)·poly(U)–drug complexes is entirely consistent with the intercalation perturbation of the phosphate ester geometry observed in the Act D and related ethidium ion complexes. The chemical shift of this downfield peak is supportive of the intercalation mode of binding, since the purely electrostatic association between drugs and nucleic acid produces only small and generally upfield ^{31}P shifts (Patel, 1979a,b; Gorenstein, 1984; Wilson & Jones, 1982). The largely unperturbed upfield signals between −1.2 and −1.6 ppm at 15 °C in these complexes likely represent undistorted phosphates in regions adjacent to the intercalation site, by analogy to our [^{17}O]phosphoryl labeling study of the [d(AGCT)]$_2$–Act D complex [Shah et al., 1984; see also Petersheim et al. (1984) for a comparable study]. The ca. 1:1 relative intensity of the downfield and main upfield peaks at saturating drug ratios is consistent with the nearest-neighbor exclusion model (Bauer & Vinograd, 1970) for these drug–duplex complexes. Thus at saturating drug ratios only every other base-pair step can accommodate an intercalated drug. According to the Jain and Sobel (1972) model, the phosphate ester backbone at the intercalation site is in an extended conformation (see below), whereas the phosphate ester backbone at the two neighboring sites is in a normal B-DNA conformation.

These results are generally comparable to our earlier ^{31}P NMR spectral study of the poly(A)·oligo(U)–Etd complex (Goldfield et al., 1983). However, in that earlier study ethidium ion stabilized the poly(A)·oligo(U) duplex, raising the melting temperature of the duplex from ca. 55 to 62 °C at saturating ethidium concentrations. In our sonicated poly(A)·poly(U) sample the melting temperature is ca. 50 °C (Figures 2 and 3). The melting temperature of the ethidium complex is essentially the same (Figure 5) although that of the daunomycin complex is ca. 56 °C. Possibly the bound ethidium drug dissociates from the duplex before melting of the duplex.

The melting of all the poly(A)·poly(U)–drug complexes shows the result of chemical exchange effects. Thus for the ethidium complex at temperatures much below T_m, the separate lines are sharp because the rate of exchange of the phosphates in the two sites (intercalation and nearest neighbor) is slow [$\tau \gg 1/(2\pi\Delta\nu)$, where τ is the lifetime of a given state and $\Delta\nu$ is the difference in chemical shift between the signals in the two states]. The lifetime of the ethidium complex is thus greater than 2 ms. Exchange between the two phosphate conformations presumably requires dissociation of the drug and rebinding at a different site. Fully resolved signals (and slow exchange conditions) are not observed in the quinacrine and daunomycin poly(A)·poly(U)–drug complex spectra, reflecting the smaller chemical shift difference between the two phosphate environments as well as possibly the shorter lifetimes for the drug complex state.

Comparison of Drug Binding to RNA and DNA Duplexes. In contrast to the above RNA duplex results, Wilson et al. (1981; Wilson & Jones, 1982) did not observe a separate downfield peak in the binding of ethidium, quinacrine, daunomycin, and tetralysine to sonicated DNA. Our own results under comparable conditions on the same DNA–drug complexes entirely confirm their earlier ^{31}P NMR studies. In both ^{31}P NMR studies on the drug–DNA complexes, increasing amounts of drugs only produce downfield shifts and line broadening. The difference between the duplex RNA and DNA systems is attributed to the rate of chemical exchange between the duplex–drug complex. In the drug–DNA complexes, under either Wilson and Jones' (1982) earlier conditions (relatively high salt, 30 °C, and magnetic field strength 24.15 MHz, ^{31}P) or our own (≥15 °C and magnetic field strength 32.38 MHz, ^{31}P), the phosphates are undergoing fast chemical exchange between sites not involving the intercalated drug (nearest neighbor or further removed) and sites directly linking the intercalated base pairs. The actual exchange of course involves the exchange of the drug between these two types of sites. Levy et al. (1984) have shown that the increase in line width upon addition of Etd is not due to a dramatic change in the motional dynamics of the complex but rather due to an increased dispersion in the ^{31}P chemical shifts. This would be consistent with an intermediate rate of chemical exchange between the intercalation and nearest-neighbor sites. The observation of intermediate/fast exchange at low field and high salt is consistent with the rates of ethidium ion binding and dissociating from DNA as measured from temperature–jump kinetic studies (Breslof & Crothers, 1975; Waring & Waring, 1980; Macgregor et al., 1985).

Even at lower temperature and slightly higher field strength, which should move the system in the direction of slow exchange kinetics, the present results on the drug–DNA complexes still show fast chemical exchange averaging (a single averaged signal; Figure 8). Indeed, the exchange kinetics of quinacrine with DNA are faster than those of ethidium while the kinetics of exchange of daunorubicin (similar to daunomycin) are slightly slower [referenced in Wilson and Jones (1982)]. However, by going to lower salt [0.01 M PIPES from the 0.2 M NaCl of this and Wilson and Jones' (1982) studies], lower temperature, and higher field strength (109.25 MHz, ^{31}P), Chandrasekaran et al. (1985) were able to demonstrate slow exchange kinetics for the ethidium–DNA complex. In this case a separate downfield shoulder is observed 1.3–1.4 ppm downfield from the main signal. Similarly, the poly(A)·poly(U)–drug complexes are clearly in slow chemical exchange on the ^{31}P chemical shift time scale. For the poly(A)·poly(U)–Etd complex we observe a well resolved downfield peak at 15 and 31 °C. For poly(A)·poly(U)–quinacrine and poly(A)·poly(U)–daunomycin, we only can see the broad downfield shift signal as a shoulder to the main sharper upfield signal, even at low temperatures.

Figures 4 and 5 illustrate nicely the effects of chemical exchange on the poly(A)·poly(U)–Etd complex. The line widths (Figure 6) remain constant, and there is little change in the separation of the signals until 50 °C when the downfield peak broadens dramatically. At $T > 50$ °C the peaks coalesce and begin to narrow again. As expected, the region of maximum line broadening occurs at intermediate chemical exchange.

A possible explanation for the large difference in the way that drugs bind to RNA [poly(A)·poly(U)] compared to DNA is that RNA double helices are more rigid than DNA double helices. Nelson and Tinoco (1984) reported that the binding of ethidium ion to duplex ribooligonucleotides is about an order of magnitude stronger than it is to duplex deoxyribooligonucleotides. The binding constant of ethidium ion is 3.5×10^4 M^{-1} at 1 °C and in 0.2 M NaCl for DNA and 4.7×10^6 M^{-1} at 25 °C and in 0.1 M NaCl for RNA (Nelson & Tinoco, 1984).

On the basis of X-ray crystallography structures for ethidium complexes with iodo-UpA and iodo-CpG, Tsai et al.

(1982) proposed a general model for ethidium binding wherein the sugar conformations are C3′(endo)–ethidium–C2′(endo). The B-form DNA generally has a C2′(endo) sugar conformation, whereas A-form RNA has a C3′(endo) conformation (Saenger, 1984). DNA can exist in a number of different conformations (A, B, alternating B, Z, etc.; Saenger, 1984), whereas the RNA structure remains predominantly A-form. Thus, the more flexible DNA may allow the ethidium to more readily dissociate from the complex.

Origin of ^{31}P Chemical Shift Perturbations in Drug Complexes. As pointed out in Ott and Eckstein (1985a,b; Connolly & Eckstein, 1984) and Schroeder et al. [1986; 1987; see also Gorenstein et al. (1988) and Gorenstein (1981, 1984)], ^{31}P chemical shifts appear to vary in response to local, sequence-specific, and induced environmental distortions in the duplex geometry (Calladine, 1982; Dickerson, 1983). Included in Figure 10 are the ^{31}P chemical shifts and helix twist values of the assigned phosphates of a number of oligodeoxyribonucleotides, as well as the chemical shifts of the drug–DNA complexes from this study and that of Wilson and Jones (1982). Wilson and Jones (1982) have noted that the ^{31}P chemical shifts of these drug complexes appear to correlate with the observed degree of unwinding of the duplex DNA upon drug binding. The helical twist values that we have used in Figure 10 from our data as well as those of Wilson and Jones (1982) represent the difference between a normal B-DNA helical twist angle of 35.6° and the observed helical unwinding angle resulting from binding of the drug. Because of the nearest-neighbor exclusion principle (Saenger, 1984), at saturating concentrations of these drugs, only every other site has a bound drug. Because of fast chemical exchange averaging, only one ^{31}P signal is observed in these drug complexes, and this must represent an average of the ^{31}P chemical shifts of phosphates at nonintercalative and intercalative sites. Correction for this chemical exchange averaging has been made in Figure 10 by multiplying the observed perturbation of the ^{31}P shifts by 2. This appears reasonable because in the poly(A)·poly(U)–drug complexes where separate ^{31}P signals for the two sites are observed the ^{31}P chemical shift of the phosphates in the intercalated drug–RNA duplexes is shifted ca. twice the amount as found for the single averaged signal in the intercalated drug–DNA duplexes [thus the poly(A)·poly(U)–Etd complex is shifted ~2.0 ppm downfield from the phosphates in the nonintercalative site and 1.7 and 2.1 ppm downfield from free poly(A)·poly(U)]. In contrast, the ^{31}P signal in the fast chemical change DNA–Etd complex is shifted 0.7 ppm downfield from the phosphates in free DNA. By going to higher field strength and lower salt, Chandrasekaran et al. (1985) were able to demonstrate slow exchange kinetics for the ethidium–DNA complex. In this case a separate downfield shoulder was observed 1.3–1.4 ppm downfield from the main signal, entirely consistent with our doubling of the observed shift in the fast exchange region. However, Chandrasekaran et al. (1985) point out that the intensity of this downfield shoulder is only ca. 15% of the total spectral area rather than the expected 50% based upon nearest-neighbor exclusion principles. Note that our slow exchange poly(A)·poly(U)–Etd spectra show that the downfield intercalated drug signal integrates for 46% of the total intensity. In other intercalative drug–oligodeoxyribonucleotide duplex complexes where large helical unwinding angles are observed and the phosphates are in slow chemical exchange, shifts of 1.5–2.5 ppm at the site of intercalation for single phosphates are also found (Patel, 1974a,b, 1976; Petersheim et al., 1984; Shah et al., 1984). Chandrasekaran et al. (1985) suggest that the deviation of their slow exchange ethidium–DNA complex could be associated with a distribution of the unwinding over several base pairs. However, our own results suggest that the decreased intensity for the downfield signal is likely associated with intermediate exchange kinetics.

The possible basis for the correlation between helix unwinding, helix twist, and ^{31}P chemical shifts in both RNA and DNA can be analyzed in terms of sugar–phosphate backbone distortions involved in duplex geometry changes (Gorenstein et al., 1988). Thus, as the helix unwinds upon binding of an intercalating drug (and the helix twist, t_g, decreases), the length of the sugar–phosphate backbone must increase to accommodate the additional heterocycle intercalated between the two stacked base pairs with a base to base separation of 6.7 Å. These local helical changes require changes in the sugar–phosphate backbone angles. This can be accomplished by the phosphate switching from the B_I ($\zeta = g^-$, $\alpha = g^-$) to the B_{II} conformation ($\zeta = t$, $\alpha = g^-$) (Dickerson, 1983). The ^{31}P signal of a phosphate in a g^-,t B_{II} conformation is predicted to be ~1.0–1.5 ppm downfield from the g^-,g^- phosphate in the B_I conformation (Gorenstein, 1981, 1984), consistent with the large downfield shift observed for the drug complexes.

Finally it should be noted that our results are consistent with the view that unwinding of the duplex upon intercalation of a drug occurs largely at the intercalated base step. In contrast, Chandrasekaran et al. (1985) have recently suggested on the basis of the low population (15%) for the downfield intercalated drug ^{31}P signal in the DNA–Etd complex that unwinding is distributed over sites adjacent to the binding site. This distribution of structural perturbation has been observed in the crystal structure of a drug–duplex complex (Quigley et al., 1980). However, the upfield ^{31}P signal representing the nearest-neighbor site is shifted very little in these RNA– and DNA–drug complexes from the chemical shift of the free duplex. This suggests little perturbation of the degree of helix twist (see Figures 10 and 11) at the nearest-neighbor site.

Conclusions

^{31}P NMR thus appears to be able to provide a convenient monitor of the phosphate ester backbone conformational changes upon binding of various intercalating drugs such as ethidium, quinacrine, and daunomycin to sonicated poly(A)·poly(U) and calf thymus DNA. The observed correlation between helix twist in DNA fragments, duplex DNA–drug complexes, and RNA–drug complexes is strongly supportive of the hypothesis that variations in P–O ester torsional angles are a major contributor to variations in ^{31}P chemical shifts.

Supplementary Material Available

Four figures showing ^{31}P NMR spectra of sonicated calf thymus DNA–ethidium complexes at various molar ratios of ethidium, ^{31}P NMR spectra of sonicated poly(A)·poly(U)–quinacrine complexes at various temperatures, ^{31}P NMR melting curves for poly(A)·poly(U)–quinacrine complexes, and ^{31}P NMR spectra of sonicated poly(A)·poly(U)–daunomycin complexes at various temperatures (5 pages). Ordering information is given on any current masthead page.

References

Akasaka, K., Yamada, A., & Hatano, H. (1975) *FEBS Lett. 53*, 339.

Akasaka, K., Yamada, A., & Hatano, H. (1977) *Bull. Chem. Soc. Jpn. 50(11)*, 2858.

Alderfer, J. L., & Hazel, G. L. (1981) *J. Am. Chem. Soc. 103*, 5925.

Anderson, J. E., Ptashne, M., & Harrison, S. C. (1987) *Nature 326*, 846–852.
Arnott, S., Hukins, D. W. L., Dover, S. D., Fuller, W., & Hudgson, A. R. (1973) *J. Mol. Biol. 81*, 107–122.
Bauer, W., & Vinograd, J. (1970) *J. Mol. Biol. 47*, 419–435.
Bontemps, J., & Fredericq, E. (1974) *Biophys. Chem. 2*, 1.
Breslof, J. L., & Crothers, D. M. (1975) *J. Mol. Biol. 95*, 103.
Calladine, C. R. (1982) *J. Mol. Biol. 161*, 343–352.
Calladine, C. R., & Drew, H. R. (1984) *J. Mol. Biol. 178*, 343–352.
Chaires, J. B., Dattagupta, N., & Crothers, D. M. (1982a) *Biochemistry 21*, 3927.
Chaires, J. B., Dattagupta, N., & Crothers, D. M. (1982b) *Biochemistry 21*, 3933.
Chandrasekaran, S., Jones, R. L., & Wilson, W. D. (1985) *Biopolymers 24*, 1963–1979.
Chen, C.-W., & Cohen, J. S. (1984) *^{31}P NMR: Principles and Applications* (Gorenstein, D. G., Ed.) Academic Press, New York.
Cohen, J. S., Wooten, J. B., & Chatterjee, C. L. (1981) *Biochemistry 20*, 3949.
Connolly, B. A., & Eckstein, F. (1984) *Biochemistry 23*, 5523–5527.
Dickerson, R. E. (1983) *J. Mol. Biol. 166*, 419–441.
Dickerson, R. E., & Drew, H. R. (1983) *J. Mol. Biol. 149*, 761–786.
Dye, J. L., & Nicely, V. A. (1971) *J. Chem. Educ. 48*, 445.
Eckstein, F., & Jovin, T. M. (1983) *Biochemistry 22*, 4546–4550.
Fratini, A. V., Kopka, M. L., Drew, H. R., & Dickerson, R. E. (1982) *J. Biol. Chem. 257*, 14686–14707.
Giessner-Prettre, C., Pullman, B., Ribas-Prado, F., Cheng, D. M., Iuorno, V., & Ts'o, P. O. P. (1984) *Biopolymers 23*, 377.
Goldfield, E. M., Luxon, B. A., Bowie, V., & Gorenstein, D. G. (1983) *Biochemistry 22*, 3336.
Gorenstein, D. G. (1978) in *Jerusalem Symposium, NMR in Molecular Biology* (Pullman, B., Ed.) pp 1–15, Reidel, Dordrecht, The Netherlands.
Gorenstein, D. G. (1981) *Annu. Rev. Biophys. Bioeng. 10*, 355.
Gorenstein, D. G. (1983a) *Bull. Magn. Reson. 5*, 161.
Gorenstein, D. G. (1983b) *Prog. Nucl. Magn. Reson. Spectrosc. 16*, 1–98.
Gorenstein, D. G., Ed. (1984) in *^{31}P NMR: Principles and Applications*, Academic Press, New York.
Gorenstein, D. G. (1987) *Chem. Rev. 87*, 1047–1077.
Gorenstein, D. G., & Kar, D. (1975) *Biochem. Biophys. Res. Commun. 65*, 1073.
Gorenstein, D. G., & Luxon, B. A. (1979) *Biochemistry 18*, 3796.
Gorenstein, D. G., & Goldfield, E. M. (1982) *Mol. Cell. Biochem. 46*, 97–120.
Gorenstein, D. G., & Goldfield, E. M. (1984) *^{31}P NMR: Principles and Applications* (Gorenstein, D. G., Ed.) Academic Press, New York.
Gorenstein, D. G., Findlay, J. B., Momii, R. K., Luxon, B. A., & Kar, D. (1976) *Biochemistry 15*, 3796.
Gorenstein, D. G., Luxon, B. A., Goldfield, E. M., Lai, K., & Vegeais, D. (1982) *Biochemistry 21*, 580.
Gorenstein, D. G., Schroder, S. A., Fu, J. M., Metz, J. T., Roongta, V., & Jones C. (1988) *Biochemistry 27*, 7223–7237.
Hogan, M. E., & Jardetzky, O. (1980) *Biochemistry 19*, 2079.
Jain, J. C., & Sobell, H. M. (1972) *J. Mol. Biol. 68*, 21.
Jones, C. R., & Kearns, D. R. (1975) *Biochemistry 14*, 2660.
Jones, R. L., & Wilson, W. D. (1980) *J. Am. Chem. Soc. 102*, 7776–7778.
Joseph, A. P., & Bolton, P. H. (1984) *J. Am. Chem. Soc. 106*, 437.
Kypr, J., Sklenar, V., & Vorlic-Kova, M. (1986) *Biopolymers 25*, 1803–1812.
Lai, K., Gorenstein, D. G., & Goldfield, E. M. (1983) *Bull. Magn. Reson. 5*, 253.
Levy, G. C., Ejchart, A., & Marchetti, P. S. (1984) *J. Magn. Reson. 57*, 130–135.
Macgregor, R. B., Clegg, R. M., & Jovin, T. M. (1985) *Biochemistry 24*, 5503–5510.
Maniatis, T., Jeffrey, A., & deSande, H. (1975) *Biochemistry 14*, 3787.
Nelson, J. W., & Tinoco, I. (1984) *Biopolymers 23*, 213.
Ott, J., & Eckstein, F. (1985a) *Biochemistry 24*, 2530–2535.
Ott, J., & Eckstein, F. (1985b) *Nucleic Acids Res. 13*, 6317–6330.
Patel, D. J. (1974a) *Biopolymers 13*, 2273.
Patel, D. J. (1974b) *Biochemistry 13*, 2388–2395.
Patel, D. J. (1974c) *Biochemistry 13*, 2396–2402.
Patel, D. J. (1976) *Biopolymers 15*, 533.
Patel, D. J. (1979a) *Biopolymers 18*, 553–569.
Patel, D. J. (1979b) *Acc. Chem. Res. 12*, 118.
Patel, D. J., & Canuel, L. L. (1979) *Eur. J. Biochem. 96*, 267–276.
Petersheim, M., Mehdi, S., & Gerlt, J. A. (1984) *J. Am. Chem. Soc. 106*, 439–440.
Reddy, B. S., Seshadri, T. P., Sakore, T. D., & Sobell, H. M. (1979) *J. Mol. Biol. 135*, 787–812.
Reinhardt, C. G., & Krugh, T. R. (1977) *Biochemistry 16*, 2890–2895.
Saenger, W. (1984) *Principles of Nucleic Acid Structure*, Springer-Verlag, New York.
Scheffler, I. E., Elson, E. L., & Baldwin, R. L. (1968) *J. Mol. Biol. 36*, 291–304.
Schroeder, S., Jones, C., Fu, J., & Gorenstein, D. G. (1986) *Bull. Magn. Reson. 8*, 137–146.
Schroeder, S., Fu, J., Jones, C., & Gorenstein, D. G. (1987) *Biochemistry 26*, 3812–3821.
Scott, E. V., Jones, R. L., Banville, D. L., Zon, G., Marzilli, L. G., & Wilson, W. D. (1988) *Biochemistry 27*, 915–923.
Shah, D. O., Lai, K., & Gorenstein, D. G. (1984) *Biochemistry 23*, 6717–6723.
Shieh, H. S., Berman, H. M., Debrow, M., & Neidle, S. (1980) *Nucleic Acids Res. 8*, 85.
Shindo, H., Simpson, R. T., & Cohen, J. S. (1979) *J. Biol. Chem. 254*, 8125.
Sundaralingam, M. (1969) *Biopolymers 7*, 821.
Tsai, C. C., Jain, S. C., & Sobell, H. M. (1982) *J. Mol. Biol. 114*, 301.
Waring, L. P., & Waring, M. (1980) *J. Mol. Biol. 144*, 183.
Wilson, W. D., & Jones, R. L. (1981) *Adv. Pharmacol. Chemother. 18*, 177.
Wilson, W. D., & Jones, R. L. (1982) *Nucleic Acids Res. 10*, 1399.
Wilson, W. D., Keel, R. A., & Miriam, R. H. (1981) *J. Am. Chem. Soc. 103*, 6267–6269.